2021-12-01

Heavy Sediment Deposition in the Yangtze Estuary, Following Initial Impoundment of Three Gorges Dam

Zhu, B

10.6937/TWC.202112/PP_69(4).0003
Taiwan Water Conservancy

臺灣水利　第**卷　第*期
民國***年*月出版

Taiwan Water Conservancy
Vol.**，No.*，*********

Heavy sediment deposition in the Yangtze Estuary, following initial impoundment of Three Gorges Dam

三峽大壩初期蓄水後長江口泥沙的大幅淤積

BOYUAN ZHU*

朱　博　淵*

School of Hydraulic and Environmental Engineering, Key Laboratory of Water-Sediment Sciences and Water Disaster Prevention of Hunan Province, Changsha University of Science & Technology, China
Lecturer

GEXUANZI LUO

羅 舸 旋 子

Changsha Institute of Mining Research, State Key Laboratory of Metal Mine Safety Technology, China
Assistant Engineer

YAO YUE

岳　遙

State Key Laboratory of Water Resources and Hydropower Engineering Science, Wuhan University, China
Associate Professor

ENHANG LIANG

梁 恩 航

The Key Laboratory of Water and Sediment Sciences, Ministry of Education; College of Environmental Sciences and Engineering, Peking University, China
Ph.D. Student

ALISTAIR G. L. BORTHWICK

School of Engineering, The University of Edinburgh, UK
Professor

YITIAN LI

李 義 天

State Key Laboratory of Water Resources and Hydropower Engineering Science, Wuhan University, China
Professor

*Corresponding author: Lecturer/School of Hydraulic and Environmental Engineering, Key Laboratory of Water-Sediment Sciences and Water Disaster Prevention of Hunan Province, Changsha university of Science & Technology/No. 960, Section 2, Wanjiali South Road, Tianxin District, Changsha City, Hunan Province, China/yuan7724@126.com

ABSTRACT

Although the initial impoundment of the Three Gorges Dam in 2003 caused a significant reduction in fluvial sediment load, heavy sediment deposition occurred within the Yangtze Estuary during 2002-2009. To gain a clear recognition of this phenomenon, the present study examines the roles of fluvial water and sediment discharges, coastal dynamics and estuarine engineering projects playing in the Yangtze estuarine erosion-deposition process. Results show that runoff discharge is the dominant factor, performing as that the alternate high and low runoff events in the Yangtze basin are associated with the cycles of morphological erosion and deposition in the Yangtze Estuary. Accordingly, the heavy deposition in the Yangtze Estuary during 2002-2009 was related to the hydrologic shift from flood events during 1997-2002 to low discharge events during 2002-2009 happened in watershed, as the landward transport of marine sediment was intensified by the relatively strengthened flood-tide force. Spatial analyses indicate that flood events in the river basin correspond to more deposition in southern subareas in the Yangtze Estuary while low discharge events correspond to more deposition in northern subareas, due to the respectively positive and negative correlations between the ebb partition ratios of north and south branching channels and runoff discharge. Therefore, the heavy deposition in the Yangtze Estuary during 2002-2009 mainly occurred in northern subareas, under the respectively significant decreases and increases in ebb partition ratios of the north and south branching channels, during the flood-to-dry hydrologic shift. As the construction of large cascade dams proceeds in the upper Yangtze, the occurrence frequency of flood events will be reduced, which is likely to cause continuous deposition in the Yangtze Estuary, with the higher amount of sediment deposited in northern subareas.

Keywords: Heavy deposition, Hydrologic shift, Erosion-deposition pattern, Ebb partition ratio, Erosion-deposition trend.

摘　　要

盡管三峽大壩 2003 年初期蓄水使得長江入海沙量顯著減少，但長江口在 2002-2009 年間發生泥沙的大幅淤積。為明晰這一現象，本文對流域水沙通量、河口動力和河口工程在長江口沖淤過程中的影響進行研究。結果表明，逕流流量是主導因素，表現為流域大小逕流事件的交替對應著長江口地貌沖淤的交替。因此，長江口 2002-2009 年間的大幅淤積源於長江流域 1997-2002 年間大洪水向 2002-2009 年間中小水的轉換，在這一過程中漲潮動力相對加強，增強了口外泥沙向口內的輸入。空間分析表明，由於長江口各汊道北邊河槽和南邊河槽的落潮分流比分別與逕流流量大小呈正相關和負相關關係，流域大、小水事件長江口的重點淤積部位分別位於南部和北部。因此，在流域大水到小水事件的轉換過程中，長江口各汊道北邊河槽和南邊河槽的落潮分流比分別顯著減小和增大，使得長江口 2002-2009 年的大幅淤積主要發生在北部。隨著長江上游大型梯級水庫建設，流域洪水事件的發生頻率降低，這將可能繼續引發長江口的淤積，並使得泥沙主要淤積在北部。

关键词：大幅淤積，水文轉換，沖淤模式，落潮分流比，沖淤趨勢。

1. INTRODUCTION

Starvation of fluvial sediment supply usually leads to erosional features in estuaries, which has been proved by the recession of shorelines and river deltas around the world over the past decades (Stanley and Warne, 1993; Milliman, 1997; Zhang *et al*., 2018; Rao *et al*., 2010). However, owing to specific factors, including dam-induced changes in hydrologic processes, coastal dynamics and estuarine engineering projects, some estuaries may also present depositional features in spite of the decrease of fluvial sediment load. Examples are as follows: 1) Water impoundment of the Youssef Ben Tachfine Reservoir led to a higher occurrence frequency of depositional lagoon condition in the Oued Massa Estuary by decreasing the frequency and magnitude of fluvial flood events (Fox *et al*., 2001). 2) Storm events caused major deposition in the Gulf of Mexico and the Mediterranean (Day *et al*., 1995). 3) Navigational improvements and regulation of wetlands triggered net sedimentation in the Columbia River Estuary over a ninety year period from 1867 to 1958 (Sherwood *et al*., 1990). In all three cases, fluvial sediment fluxes decreased.

The Yangtze Estuary (Figures 1a and b), the largest estuary in China, also underwent deposition in its mouth bar area (the area given by A+B+C+D in Fig.1b) during 2002-2009 when the fluvial sediment load (recorded at Datong Hydrological Station, Fig.1a) declined by nearly 70% after the initial impoundment of the TGD (Fig.1a), the largest river dam in the world, in 2003 (Dai *et al*., 2014). Compared with the average depositional rate in the area during 1958-2002, the data during 2002-2009 approximately doubled (Dai *et al*., 2014), especially remarkable over 2002-2004, which was much higher than many other estuaries, such as the three examples described previously (Sherwood *et al*., 1990; Day *et al*., 1995; Fox *et al*., 2001). What is the mechanism behind this heavy deposition? Dai *et al.* (2014) argued that it occurred because river regulation by the TGD lowered the occurrence frequency of peak fluvial flood events and in turn enhanced the delivery of offshore sediment to the estuary, and the coastal dynamics also changed within the same period (waves, currents, storm surges, etc.). This argument however neglected the role of an important natural event whereby a hydrologic shift from flood events (prevalent during 1997-2002, especially 1998 and 1999 when the Yangtze River experienced severe floods) to low discharge events (during 2002-2009) occurred, which caused a greater reduction in peak fluvial flood discharge than that due to the limited river-regulation operations by the TGD during its initial impoundment stage (Dai *et al*., 2008; Li *et al*., 2013). Dai *et al*. (2014) also analyzed the migratory track of the depocenter (where the depositional rate was maximal in the Yangtze Estuary) and pointed out that the depocenter moved towards the opening of the branching channel where the sediment partition ratio (defined as the suspended sediment load

in a given branching channel divided by the total suspended load of the upstream river channel) was the highest (in comparison with all other branching channels). However, during 2007-2009, the depocenter moved to the opening of the North Channel (Fig.1b) rather than the South Passage (Fig.1b) even when sediment partition ratio of the latter exceeded 50% (Dai *et al*., 2014). Therefore, the mechanism behind the heavy deposition in the Yangtze Estuary has not been revealed thoroughly.

This study aims to provide a complete understanding of the heavy deposition in the Yangtze Estuary and predict the erosion-deposition trend. A comprehensive analysis on the effects of possible factors was carried out on the basis of relevant data of fluvial water and sediment discharges, marine sediment supply, coastal dynamics, estuarine engineering projects, water excavating force in branching channels and terrain of the estuary. Our findings may be helpful in designing future navigational projects and planning land resources in the Yangtze Estuary, and applicable to other estuaries in the world.

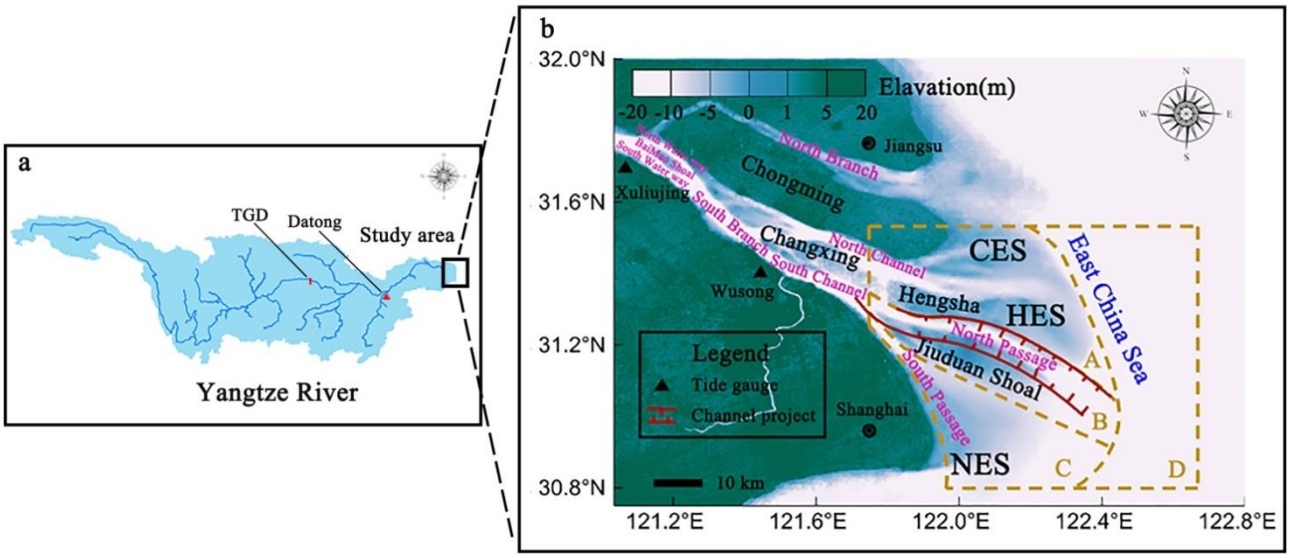

Fig.1. Location and key features of the Yangtze Estuary. (a) Locations of the Yangtze Estuary, TGD and Datong Station. (b) Plan view of the Yangtze Estuary.

2. GEOGRAPHICAL SETTING

The Yangtze Estuary is the largest estuary in China, with 180 km in length from west to east and 6-90 km in width from north to south. The main channels of the Yangtze Estuary undergo four-fold bifurcations (Fig.1b): at Chongming Island, the river divides into the North Branch and the South Branch; the South Branch almost immediately branches to pass Baimao Shoal and splits as North Waterway and South Waterway, with the branches reconnecting after the shoal; at Changxing and

Hengsha Island, the South Branch again bifurcates, forming the North Channel and the South Channel at Changxing Island; at the Jiuduan Shoal, the South Channel divides into the North Passage and the South Passage. Four non-overlapping subareas A, B, C and D of interest are marked on the diagram (Fig.1b), which are the same as those concerned by Dai *et al*. (2014). Subarea A covers the eastern reach of the North Channel, subarea B covers the North Passage, subarea C covers the South Passage and subarea D is located in the East China Sea, immediately to the east of A, B and C. Three tidal flats, namely, Chongming east shoal, Hengsha east shoal and Nanhui east shoal, are located at the front edge of the estuary; they are abbreviated to CES, HES and NES, respectively (Fig.1b). The Yangtze Estuary is meso-tidal with a mean tide range of 2-3 m and flow velocity of about 1 m/s (Li *et al*., 2011; Zhang *et al*., 2016)

3. DATA AND METHODS

3.1 Data sources

Datong Hydrological Station (thereafter Datong) is the last hydrological station which has the long-term water and sediment discharge records in the Yangtze River. It is about 500 km upstream from the Yangtze Estuary (Fig.1a). There is no major tributary downstream of Datong (Fig.1a) and the runoff time series approximate those at Xuliujing (Zhu *et al*., 2017) which is located at the upper entrance of the Yangtze Estuary (Fig.1b); therefore, the water and sediment discharge records at Datong can represent those flowing into the Yangtze Estuary. Observed daily water discharge time series from 1923 to 2016 at Datong were supplied by the Changjiang Water Resources Commission.

Besides, the following data were collected from published literature (Table 1): 1) Data of storm surge in the Yangtze Estuary over the past 50 years 2) Data of ebb partition ratios in branching channels in the Yangtze Estuary. Here, the ebb partition ratio of a *j*-th branch in a *i*-th bifurcation is defined as the ebb flow discharge in the *j*-th branch divided by the total ebb discharge immediately upstream of the *i*-th river node where bifurcation occurs, and is verified as an effective index for representing water excavation force in branching channels in the Yangtze Estuary (Zhu *et al*., 2017). 3) Data that reflect the variations of net sediment fluxes at Datong, Xuliujing and Yangtze River mouth. 4) Terrain data include the volume change rates (thereafter *VCR*, unit: $m^3\ yr^{-1}$) in subareas A, B, C and D, the channel volume of the North Passage and the South Passage, the amount of dredging sludge of the channel project in the North Passage, the amount of dredging sludge swept onto the Hengsha east shoal and the amount of land reclamation at tidal flats.

Table 1. Data collected from published literature

Data type	Data name	Source
Coastal dynamics	Storm surge	Dai *et al*., 2014
Water excavating force in branching channels	Ebb partition ratios in branching channels	Yun, 2004; Yang, 2014; Dai *et al*., 2016; Wu, 2017; Dao *et al*., 2018
Sediment supply	Sediment load at Datong, Xuliujing and Yangtze river mouth	Yang *et al*., 2014
Terrain	*VCR* in subareas A, B, C and D	Dai *et al*., 2014
	Channel volume of the North Passage and the South Passage	Gao *et al*., 2009
	Amount of dredging sludge of the channel project in the North Passage	Liu, 2008; Luan *et al*., 2016
	Amount of dredging sludge swept onto the Hengsha east shoal	Xu and Zhu, 2009
	Amount of land reclamation at tidal flats	Du *et al*., 2013

3.2 Interpretation of runoff discharge

From the daily river water discharge time series at Datong, the number of days in which the discharge exceeded 60,000 m^3/s (thereafter $D_{60,000}$) during any year was counted to reflect the severity of fluvial flood events during the periods of interest. Herein, 60,000 m^3/s was adopted as a critical discharge because it is higher than the multi-year average peak-flood of 58,449 m^3/s (calculated using the daily water discharge time series from 1950 to 2016) at Datong and approaches the effective/bankfull discharge (Andrews, 1980; Emmett and Wolman, 2001; Gomez *et al*., 2007; Xia *et al*., 2014) of 60,400 m^3/s which plays the key role in morphological changes in the Yangtze Estuary (Yun, 2004). Annual mean duration days of different runoff discharge levels were also calculated in order to depict the variability of runoff discharge more precisely.

3.3 Modification of *VCR* allowing for channel projects in North Passage

In 1984, the main shipping channel of the Yangtze Estuary was constructed in the North Passage. To maintain navigational functionality of 7 m depth and 250 m width, 12×10^6 m^3 of sludge was dredged along the 16 km long channel every year from 1984 to 1997 (Liu, 2008). In 1998, the Deepwater Channel Project commenced, aimed at deepening the channel to 12.5 m. An increased amount of sediment then

became trapped in the North Passage under the joint influence of river flow, waves and wind (Song and Wang, 2013; Song *et al*., 2013), and therefore the yearly quantity of dredging sediment had to be raised (Liu, 2008). Before 2004, dredging sludge was dumped offshore (Liu, 2008); after 2004, however, part of the dredging sludge was supplied to the Hengsha east shoal (within subarea A, Fig.1b), with the remainder disposed offshore of the coast (within subarea D, Fig.1b) (Liu, 2008; Xu and Zhu, 2009). Since the deposition of the huge amount of dredging sludge from the North Passage greatly disturbed the erosion-deposition in the surrounding area, *VCR* in the subareas A, B, C and D should be modified based on the dredging amount to restore the morphological changes. The *VCR* (deposition positive, erosion negative) corresponding to the subareas are modified as follows:

$$VCR'_A = (VCR_A \cdot T - V_A) / T \quad (1)$$

$$VCR'_B = (VCR_B \cdot T + V_B) / T \quad (2)$$

$$VCR'_D = [VCR_D \cdot T - (V_B - V_A)] / T \quad (3)$$

where VCR_A, VCR_B, and VCR_D (m^3/yr) are the original *VCR* in subareas A, B, and D; VCR_A', VCR_B' and VCR_D' (m^3/yr) are the modified *VCR* in subareas A, B, and D; T (yr) is the time span; V_B (m^3) represents the total volume of sludge dredged from the North Passage (within subarea B); V_A (m^3) represents the volume of dredging sludge swept onto the Hengsha east shoal (within subarea A). The *VCR* in subarea C remains unmodified because it was not affected by the dredging sludge. As the amount of sediment balances within the four subareas during the process of modification, *VCR* of the whole area of A+B+C+D keeps consistent before and after the modification. Table 2 lists the values of parameters used to calculate the modified *VCR*.

Table 2. Parameters for modifying *VCR* in the subareas, considering the impacts of channel projects in the North Passage

Period	Subarea	*VCR* [a] (10^6 m^3/yr)	*VCR*' (10^6 m^3/yr)	*T* (yr)	V_B [b] (10^6 m^3)	V_A [c] (10^6 m^3)
1958-1978	A	37	37	20	0	0
	B	57	57			
	D	143	143			
1978-1989	A	25	25	11	60	0
	B	12	17.5			
	D	-34	-39.5			
1989-1997	A	0.62	0.62	8		0

	B	56	68		96	
	D	-39	-51.6			
	A	-7.6	-7.6			0
1997-2002	B	-16	5	5	105.4	
	D	-34	-55.4			
	A	184	176			15.1
2002-2004	B	7	37	2	60	
	D	166	144			
	A	19	-8			81.2
2004-2007	B	109	154.6	3	136.8	
	D	52	34.8			
	A	87.5	61.5			52.4
2007-2009	B	-50	6.7	2	113.9	
	D	17	-14.2			

[a] Source: Dai *et al*., 2014.

[b] Source: Liu, 2008.

[c] Source: Xu and Zhu, 2009.

3.4 Calculation of thickness change rate

Considering the different acreages of subareas A, B, C and D, *VCR* cannot well reflect the difference in the erosion-deposition intensity among the subareas. Therefore, the thickness change rates (thereafter *TCR*, unit: m/yr) in the subareas were calculated through dividing *VCR* (m^3/yr) in the subareas by the acreages (m^2) of the subareas. The calculating equation is shown as follow:

$$TCR = VCR' / S \qquad (4)$$

where *TCR* represents the thickness change rate (m/yr) of each subarea, *VCR'* represents the modified *VCR* (m^3/yr) of each subarea in Table 2, *S* represents the acreage (m^2) of each subarea, of which *S* of the subareas were worked out through the following three steps: first, the geographic coordinates (^{o}E and ^{o}N) of defined points were acquired along the outlines of the subareas A, B, C and D in Dai *et al*. (2014) using the Getdata Gragh Digitizer; second, these coordinates were translated into lengths (m) using a coordinate converter (i.e. Coor, developed by the Shanghai Estuarine & Coastal Science Research Center, China); thirdly, the subareas were redrawn based on the defined points with coordinates of lengths along the outlines in AutoCAD and then the acreages (m^2) of the subareas could be evaluated using AutoCAD. Relevant parameters relating to the calculation of *TCR* in the subareas are listed in Table 3.

Table 3. Parameters for calculating *TCR* in the subareas

Period	Parameter	Subarea				
		A	B	A+B	C	D
	S (10^6 m^2)	1712	1075	2787	1181	2342
1958-1978	*VCR'* (10^6 m^3/yr)	37	57	94	24	143
	TCR (mm/yr)	21.6	53.0	33.7	20.3	61.1
1978-1989	*VCR'* (10^6 m^3/yr)	25	17.5	42.5	-1	-39.5
	TCR (mm/yr)	14.6	16.3	15.2	-0.8	-16.9
1989-1997	*VCR'* (10^6 m^3/yr)	0.62	68	68.6	1	-51.6
	TCR (mm/yr)	0.3	63.2	24.6	0.8	-22.0
1997-2002	*VCR'* (10^6 m^3/yr)	-7.6	5	-2.6	18	-55.4
	TCR (mm/yr)	-4.4	4.6	-0.9	15.2	-23.7
2002-2004	*VCR'* (10^6 m^3/yr)	176	37	213	125	144
	TCR (mm/yr)	102.8	34.4	76.4	105.8	61.5
2004-2007	*VCR'* (10^6 m^3/yr)	-8	154.6	146.6	0.67	34.8
	TCR (mm/yr)	-4.7	143.7	52.6	0.6	14.9
2007-2009	*VCR'* (10^6 m^3/yr)	61.5	6.7	68.2	-9	-14.2
	TCR (mm/yr)	35.9	6.2	24.5	-7.6	-6.1

[a] The magnitude of *TCR* (mm/yr) in this table is the same as that in previous studies (Dai *et al*., 2014; Luan *et al.*, 2016; Zhao *et al*., 2018), implying a good reliability of the terrain data.

4. RESULTS

4.1 Relationship between total *VCR* of the subareas and runoff discharge

Fig.2a indicates two cycles of *VCR* covering area A+B+C+D: one began with erosion during the period around 1954 (Although no information was available on the *VCR* before 1958, the erosion of Yangtze mouth bar area, including the formation of the North Passage, around 1954, provided convincing evidence for the erosion (Wu *et al*., 2003; Yun, 2004; He *et al*., 2013), proceeding with heavy deposition during 1958-1978 and then gradually decreasing deposition from 1978 to 1997; the other started with erosion during 1997-2002, progressing with heavy deposition during 2002-2004 and then gradually decreasing deposition from 2004 to 2009.

Through the comparison with runoff condition in Fig.2b, it can be seen that each cycle of *VCR* commenced in a period with a high value of $D_{60,000}$, such as the periods

contained the flood years of 1954 and 1998 which experienced the peak values of $D_{60,000}$ (and also the yearly water discharge). That is to say, erosion occurred with high $D_{60,000}$ (and also the yearly water discharge) events first, then the heavy deposition and gradually decreasing deposition happened with the following low values of the runoff indexes.

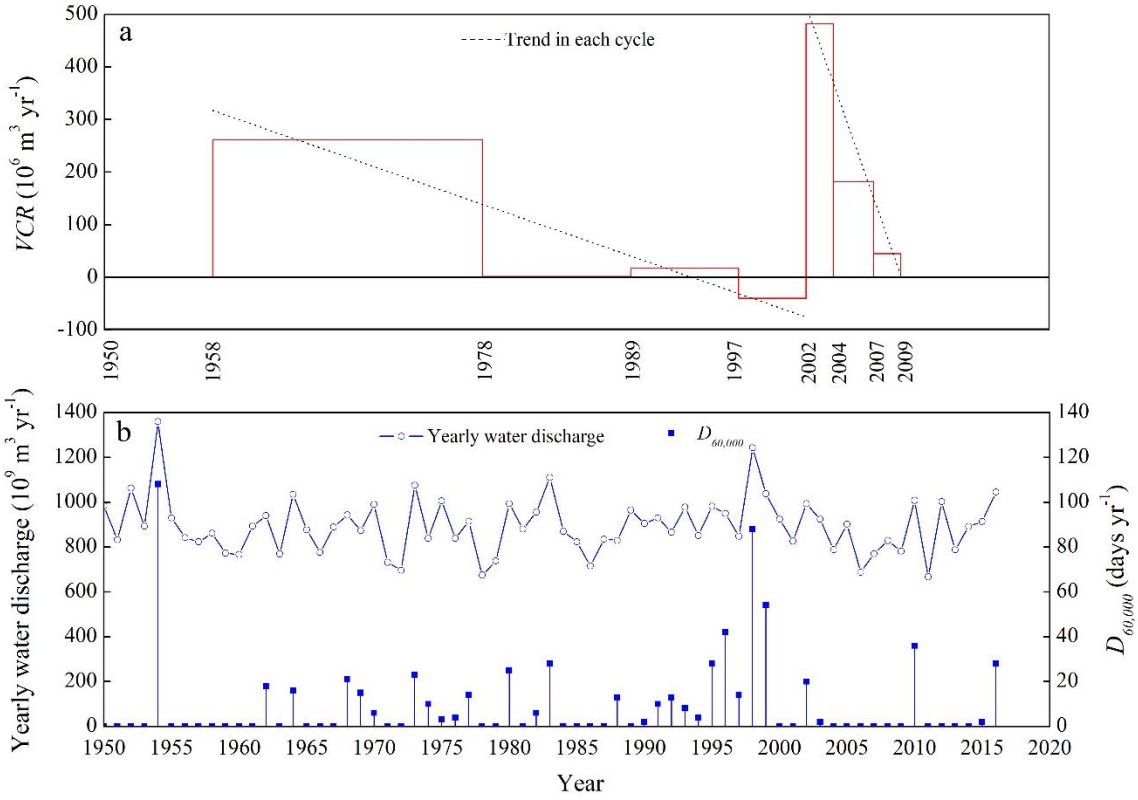

Fig.2. Morphology-runoff processes in the Yangtze Estuary. (a) Histogram of *VCR* (deposition positive, erosion negative) summed over the four subareas A, B, C and D (indicated in Fig.1b) for the following periods: 1958–1978, 1978–1989, 1989–1997, 1997–2002, 2002–2004, 2004–2007 and 2007–2009. Superimposed are two regression lines, one for the overall period from 1958 to 2002, and the other from 2002 to 2009. (b) Yearly water discharge and duration days of high-level discharge events (>60,000 m^3/s) at Datong from 1950 to 2016.

4.2 Relationship between spatial erosion-deposition pattern of the subareas and runoff discharge

Fig.3 shows that during the period of 1997-2002 with the highest value of $D_{60,000}$, *TCR* in the northern subareas A and B were lower than that in the southern subarea C; while during other periods with low values of $D_{60,000}$, the situation was generally inverse, except the case during the period of 2002-2004. This kind of phenomenon means that the northern subareas tend to experience more deposition than the southern subareas under low runoff intensities, while less deposition under high runoff intensities. As a result, during the period

of 2002-2009 with low values of $D_{60,000}$, the heavy deposition mainly occurred at northern subareas A and B, performed as the higher *TCR* in subarea A+B (0.051 m/yr) and the lower *TCR* in subarea C (0.028 m/yr) (calculated using the data in Table 3).

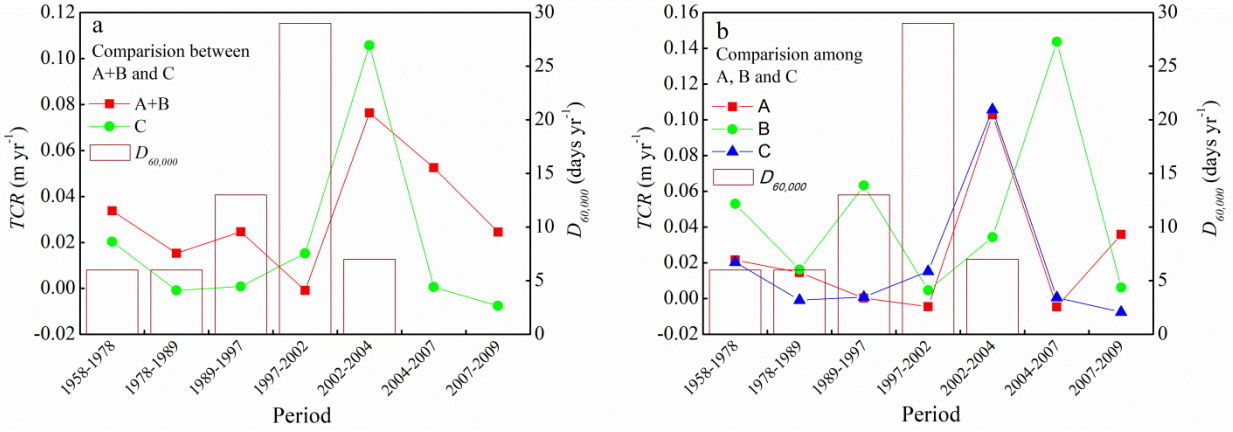

Fig.3. Comparison of *TCR* (deposition positive, erosion negative) for subareas A, B and C with varying $D_{60,000}$. (a) Comparison between A+B and C. (b) Comparison among A, B and C.

Further evidences for this kind of erosion-deposition discrepancy between the northern and southern subareas in the Yangtze Estuary are provided by the channel thalwegs. It can be seen from Fig.4 that the thalwegs of the north branching channels (North Channel and North Passage) were enhanced and lengthened during low $D_{60,000}$ events, and lowered and shortened during high $D_{60,000}$ events, whereas the situation for the thalweg of the south branching channel (South Passage) was quite the opposite.

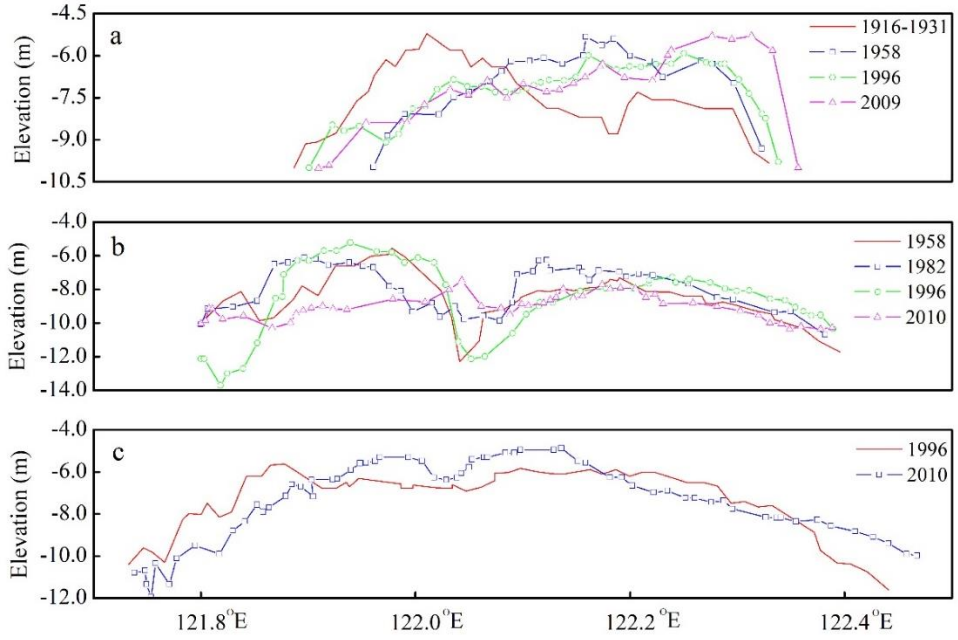

Fig.4. Evolution of thalwegs in the North Channel, North Passage and South Passage of the Yangtze Estuary. Thalweg elevation refers to the theoretical low-tide datum at Wusong (Fig.1b). (a) Evolution of the thalweg in the North Channel from 1916–1931 to 1958 with $D_{60,000}$ =16 days/yr, from 1958 to 1996 with $D_{60,000}$ = 8 days/yr and from 1996 to 2009 with $D_{60,000}$ = 16 days/yr. (b) Evolution of the thalweg in the North Passage from 1958 to 1982 with $D_{60,000}$ = 6 days/yr, from 1982 to 1996 with $D_{60,000}$ = 10 days/yr and from 1996 to 2010 with $D_{60,000}$ = 17 days/yr. (c) Evolution of the thalweg in the South Passage from 1996 to 2010 with $D_{60,000}$ = 17 days/yr.

5. DISCUSSION

5.1 Mechanism behind the heavy deposition

5.1.1 Major role of runoff discharge and sediment source

Comparison between the two subseries of *VCR* in area A+B+C+D and the runoff process at Datong (Fig.2) indicates that runoff discharge played a major role in determining the erosion-deposition cycles in the Yangtze Estuary. Under the backdrop of stable offshore tidal dynamics (tidal range) in the Yangtze Estuary at the yearly time-scale (Dai *et al*., 2014; Zhu *et al*., 2017), during periods with high runoff discharge, the ebb-tide flow is relatively stronger than the flood-tide flow, thereby the river bed is eroded by the ebb-tide flow and sediment is delivered into the offshore area; in following periods with low runoff discharge, the ebb-tide flow is relatively weaker than the flood-tide flow, and a considerable amount of sediment is taken from the offshore area into the estuary, leading to heavy deposition. As the deposition approaches equilibrium, *VCR* decreases, until the next flood event comes and produces erosion again.

To prove that the flood-tide-driving sediment transport from the offshore area provided the main material source for the heavy deposition, the sediment balance in the Yangtze Estuary is analyzed. Table 4 shows that net sediment fluxes at Datong, Xuliujing and the river mouth all decreased from 1958-1993 to 2003-2009, and the river bed between Datong and Xuliujing changed from depositional state to erosional state, while the river bed between Xuliujing and river mouth kept depositional state all the time. The decreases of net sediment fluxes at the three cross-sections indicated a declining trend of fluvial sediment load entering the Yangtze Estuary, which was not corresponding to the events of heavy deposition in the two sub-series of *VCR* in area A+B+C+D (Fig.2a). More precisely, during 2003-2009, if assuming that all the sediment load at Xuliujing deposited only within area A+B+C+D, which highly overestimates the deposition rate, it only results in *VCR* about 65×10^6 m^3/yr (the density of sediment is adapted as 2.65 t/m^3), significantly less than the measured average *VCR* of 229×10^6 m^3/yr (calculated using the data in Fig.2a from 2002 to 2009) during the period. In fact, the deposited amount in area A+B+C+D contributed by fluvial sediment was

even far less than 65×10^6 m^3/yr considering the depositional state between Xuliujing and the river mouth during that period (Table 4). Hence, the sediment of the heavy deposition in area A+B+C+D during 2002-2009 should mainly come from the offshore area, rather than the watershed.

Table 4. Net sediment fluxes at key cross-sections and erosion-deposition amounts in relevant reaches

Period	Net sediment flux (10^8 t/yr)			Erosion-deposition amount (10^8 t/yr)	
	Datong	Xuliujing	River mouth	Datong-Xuliujing	Xuliujing-River mouth
1958-1993	4.51	4.06	3.70	0.45	0.36
1991-2002	3.27	2.94	2.76	0.33	0.18
2003-2009	1.47	1.71	1.25	-0.24	0.46

Above analyses indicate that the heavy deposition in the Yangtze Estuary during 2002-2009 (especially 2002-2004) was mainly related to a hydrologic shift from river flood discharge to low discharge, with the deposited sediment mainly came from the offshore area. The TGD started to impound water in 2003, and he significant decrease in duration days of high discharge (> 50,000 m^3/s) and increase in duration days of low discharge (10,000 - 20,000 m^3/s) from 1950-2002 to 2003-2016 (Fig.5) indicate that water regulation by TGD is high likely to have contributed to the hydrologic shift and helped aggravate the deposition concerned over a multi-year timescale, although the effect was limited during the initial impoundment of TGD (Dai *et al*., 2008; Li *et al*., 2013).

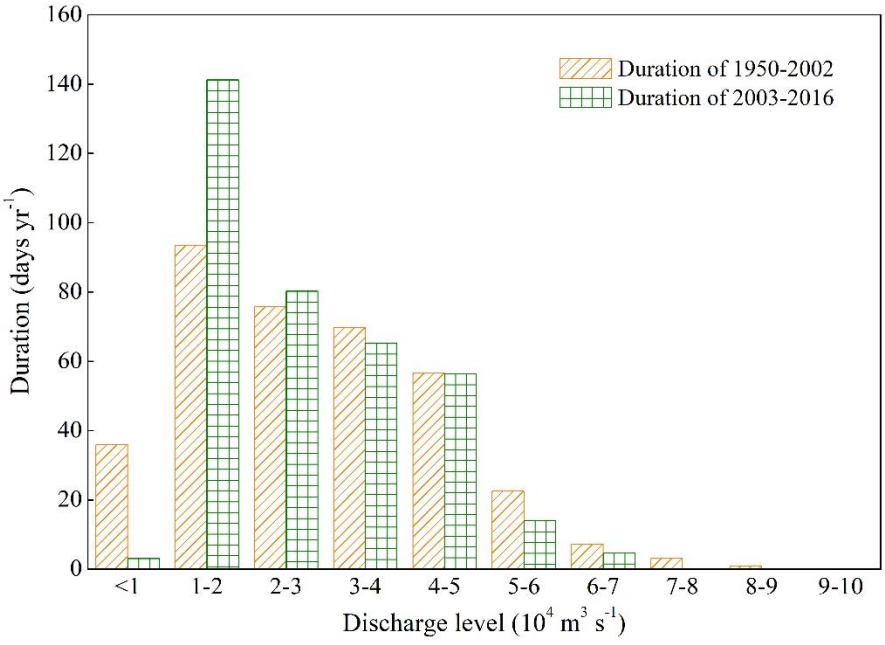

Fig.5. Histogram of annual average duration days of different runoff discharge levels at Datong before TGD impoundment (1950–2002) and after (2003–2016).

5.1.2 Roles of other possible factors

Coastal dynamics. Typhoon-induced storm surge acts as a random forcing factor. Over the past 50 years, several typhoon incidents have occurred in the Yangtze Estuary (Fig.6a). Although storm surges severely erode estuaries (Ren *et al*., 1985; Yang *et al*., 2003; Rangel-Buitrago and Anfuso, 2011; Crapoulet et al., 2017; van Puijenbroek et al., 2017), the depositional recovery from such erosion is usually substantial within one or several weeks (Ren *et al*., 1985; Yang *et al*., 2003). Hence, storm surges in the years before 2002 (Fig.6a) should not have caused the heavy deposition in area A+B+C+D observed during 2002-2009 (especially 2002-2004). Moreover, these storm surges were more powerful (Fig.6a), leading to more transient erosion and higher short-term depositional recoveries than that in 2002, and therefore the storm surge in 2002 with weaker energy (Fig.6a) also should not have incurred the heavy deposition. Waves and littoral currents are classed as wind-driven environmental forcing factors in estuaries (Shepard, 1963; Grady *et al*., 2013). In the subtropical monsoon climate zone, such as the Yangtze Estuary, seasonal variations in wind magnitude and direction cause associated seasonal cycles in waves and littoral currents. A morphological balance is hence established in the Yangtze Estuary on a yearly basis (Ji and Jiang, 1994; Guo *et al*., 2003), rather than on a decadal basis through erosion-deposition cycles (Fig.2a). It should also be noted that continuous sea level rise has facilitated very long-term progressive erosion in the Yangtze Estuary ever since the estuary formed (Ji and Jiang, 1994; Yang *et al*., 2000; Zhou *et al*., 2013), and so is not a factor regarding the heavy deposition in the Yangtze Estuary as well.

Estuarine engineering projects. The largest navigational project in the Yangtze Estuary, the Deepwater Channel Project, was implemented in 1998 in the North Passage (Fig.1b). Although this project has been associated with notable deposition in its vicinity, primarily in the North Passage (Liu, 2008; Song and Wang, 2013; Song *et al*., 2013; Luan *et al*., 2016), the deposition did not occur until 2004 (Fig.6b), later than the heavy deposition during 2002-2004 in the area A+B+C+D; furthermore, deposition after 2004 has presented an upward trend (Fig.6b), which was not in accord with the gradually decreasing deposition in area A+B+C+D from 2004 to 2009. Consequently, the Deepwater Channel Project was most unlikely to be the cause of the deposition in area A+B+C+D during 2002-2009. Reclamation is another important human activity in the Yangtze Estuary, which has expanded the land area of Shanghai City (Fig 1a) by 20% over the past 60 years (Wei *et al*., 2015), and has mainly been carried out at two areas: the tidal flats and the North Branch (Du *et al*., 2013; Wei *et al*., 2015; Dai *et al*., 2016). At the tidal flats, reclamation activities

may have affected the erosion-deposition balance in the area A+B+C+D, owning to the major partial overlap between the tidal flats and the area (Fig.1b). Fig.6c shows the acreage of reclaimed land per year recorded at the tidal flats over the past few decades. There appeared to be no abrupt increase in reclamation acreage at each tidal flat during 2002-2004, suggesting that land reclamation had not contributed to the heavy deposition in area A+B+C+D. A more detailed comparison between Figures 2a and 6c confirms the lack of connectivity between *VCR* in area A+B+C+D and the acreage of reclaimed land.

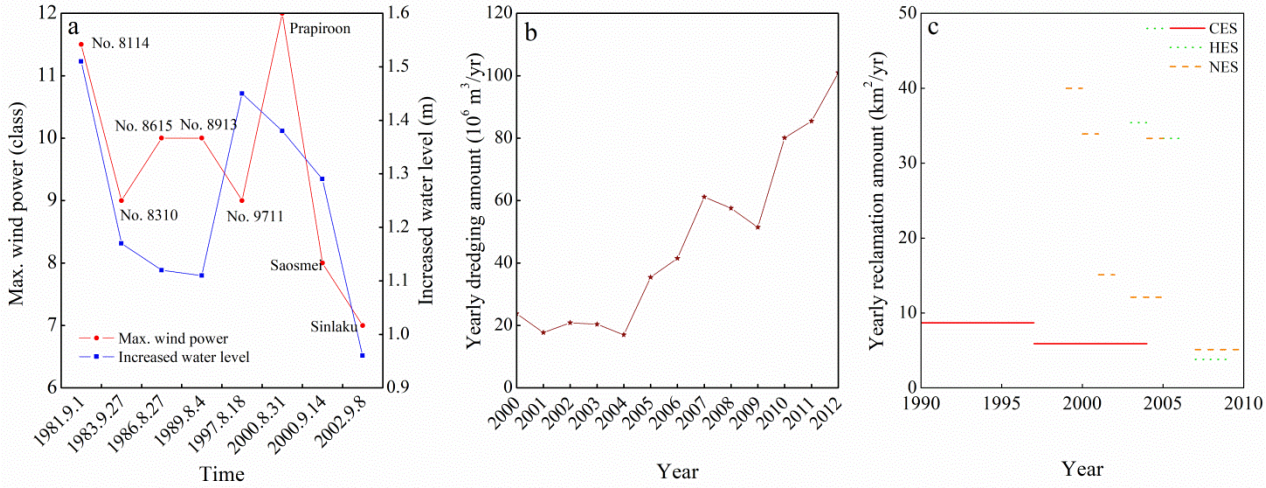

Fig.6. Coastal dynamics and engineering projects in the Yangtze Estuary. (a) Strength of major typhoon-induced storm surges over the past 50 years in the Yangtze Estuary. (b) Yearly dredging amount of the Deepwater Channel Project in the North Passage. (c) Reclamation acreage per year at tidal flats during 1990-2010. Locations of CES, HES and NES are shown in Fig.1b.

5.2 Mechanism behind the spatial erosion-deposition pattern

On account of the difference of bed elevation between north and south branching channels and the northeastward raised nodes along the south bank of the Yangtze Estuary, the ebb partition ratios in the North Branch, North Waterway of Baimao Shoal, North Channel and North Passage increase as runoff discharge rises, whereas those of the South Branch, South Waterway of Baimao Shoal, South Channel and South Passage decrease (Zhu *et al.*, 2017). This is further supported by the higher values of ebb partition ratios in the north branching channels during the periods with high values of $D_{60,000}$ than those with low values of $D_{60,000}$ and the reverse situation for the south branching channels (Table 5). The periods in Table 5 contain the hydrologic-shift period (from 1997-2002 to 2002-2009) concerned in this study.

Table 5. Multi-year average ebb partition ratios in the branching channels of the four bifurcations in the Yangtze Estuary during different periods with corresponding multi-year average values of $D_{60,000}$

Bifurcation	Ebb partition ratio (%)		$D_{60,000}$ (days yr^{-1})	Period
	North branching channel [a]	South branching channel [a]		
First bifurcation	-1.58 [b]	101.58	6	1958-1978
	-1.30 [b]	101.30	6	1978-1989
	3.65	96.35	13	1989-1997
	3.66	96.34	29	1997-2002
	-10.30 [b]	110.30	6	2002-2011
Second bifurcation	37.58	62.42	7	2002-2004
	34.62	65.38	0	2004-2007
	33.40	66.60	0	2007-2009
	31.60	68.40	12	2009-2011
	29.50	70.50	0	2011-2013
Third bifurcation	48.17	51.83	6	1978-1989
	51.10	48.90	13	1989-1997
	52.17	47.83	29	1997-2002
	49.12	50.88	4	2002-2007
Fourth bifurcation	54.83	45.17	29	1997-2002
	50.07	49.93	7	2002-2004
	47.93	52.07	0	2004-2007
	43.30	56.70	0	2007-2009

[a] The north/south branching channel of the four bifurcations are North/South Branch, North/South Waterway of Baimao Shoal, North/South Channel and North/South Passage respectively.

[b] The negative value of ebb partition ratio in the North Branch implied that the flood-tide current overwhelmed the ebb-tide one during those three periods, which incurred the backward flow in the North Branch from the sea to the upper boundary (i.e. Xuliujing in Fig. 1b) and the flow then entered into the South Branch (Dai *et al*. 2016).

Given that the yearly ebb-tide discharge is approximately constant in the Yangtze Estuary (Zhu *et al*., 2017), more ebb-tide flow is distributed to the south branching channels and less ebb-tide flow is distributed to the north branching channels during the periods with low

values of $D_{60,000}$, while the completely opposite situation happens during the periods with high values of $D_{60,000}$. Thus, during the periods (such as 2002-2009 concerned) with low values of $D_{60,000}$, the ebb-tide force in the south branching channels (South Branch, South Waterway of Baimao Shoal, South Channel and South Passage) is strong, weakening the flood-tide force in southern subareas and washing the sediment into the sea, leading to erosion or reduced deposition in southern subareas (e.g., C, located south of the Jiuduan Shoal, Figures 3 and 4); meanwhile, the ebb-tide force in the north branching channels (North Branch, North Waterway of Baimao Shoal, North Channel and North Passage) is weak, the flood-tide force in northern subareas is then relatively reinforced and brings more sediment from the offshore area into northern subareas, resulting in deposition or less erosion in northern subareas (e.g., A and B, located north of the Jiuduan Shoal, Figures 3 and 4). During the periods with high values of $D_{60,000}$, reverse situation happens between the northern and southern subareas (Figures 3 and 4). The outlier situation during 2002-2004 in Fig 3 (with *TCR* in A and B smaller than that in C accompanied by low value of $D_{60,000}$) might be related to the increased ebb partition ratios in the south branching channels upstream of the subareas A, B, C and D, which washed sediment in upstream southern subareas into C, in view of the relationship between ebb partition ratio and runoff discharge (Zhu *et al*., 2017).

5.3 Erosion-deposition trend

5.3.1 Trend of total erosion-deposition

After the TGD became operational in 2003, the occurrence frequency of high-level runoff discharge decreased greatly (Fig.5), and so the cycles of alternate erosion and deposition that previously characterized the Yangtze Estuary were interrupted, replaced by maintained deposition of the sediment from offshore area. Observations during 2002-2009 showed that the mean *VCR* after the impoundment of TGD were 86×10^6 m^3/yr in subarea A, 34×10^6 m^3/yr in subarea B, 33×10^6 m^3/yr in subarea C and 75×10^6 m^3/yr in subarea D (calculated using the data in Dai et al., 2014), which provided the evidence confirming the maintained deposition. At the time of writing, a cascade of large dams is consecutively under construction along the upper Yangtze, and it is likely that the frequency of large river flood events will continue to be reduced due to water regulation by the dams (Duan *et al*., 2016). Therefore, the deposition is most likely to persist in the Yangtze Estuary for the near future.

5.3.2 Trend of spatial erosion-deposition pattern

In addition to the trend of total sediment deposition in the Yangtze Estuary, the reduction in occurrence frequency of river flood events will encourage more sediment deposition in the northern subareas than the southern subareas, under the effect of the decreasing trend of ebb partition ratios in the north branching channels and the increasing

trend of ebb partition ratios in the south branching channels, based on the relationship between ebb partition ratio and runoff discharge (Zhu *et al.*, 2017). Hence, current discrepancy of erosion-deposition between northern and southern subareas in the Yangtze Estuary will be sustained. Fig.7 illustrates the changes in channel volume of the North and South Passages from 2003 to 2008. While the North Passage decreased in volume from 3100×10^6 m^3 to 2800×10^6 m^3 after the impoundment of TGD, the volume of the South Passage increased from 1423×10^6 m^3 to 1439×10^6 m^3 in the same period, in accordance with the predicted trend. The change trends of volume in north and south branching channels in the Yangtze Estuary given by Zhu *et al.* (2017) further demonstrate the difference of erosion-deposition trends between the northern and southern subareas.

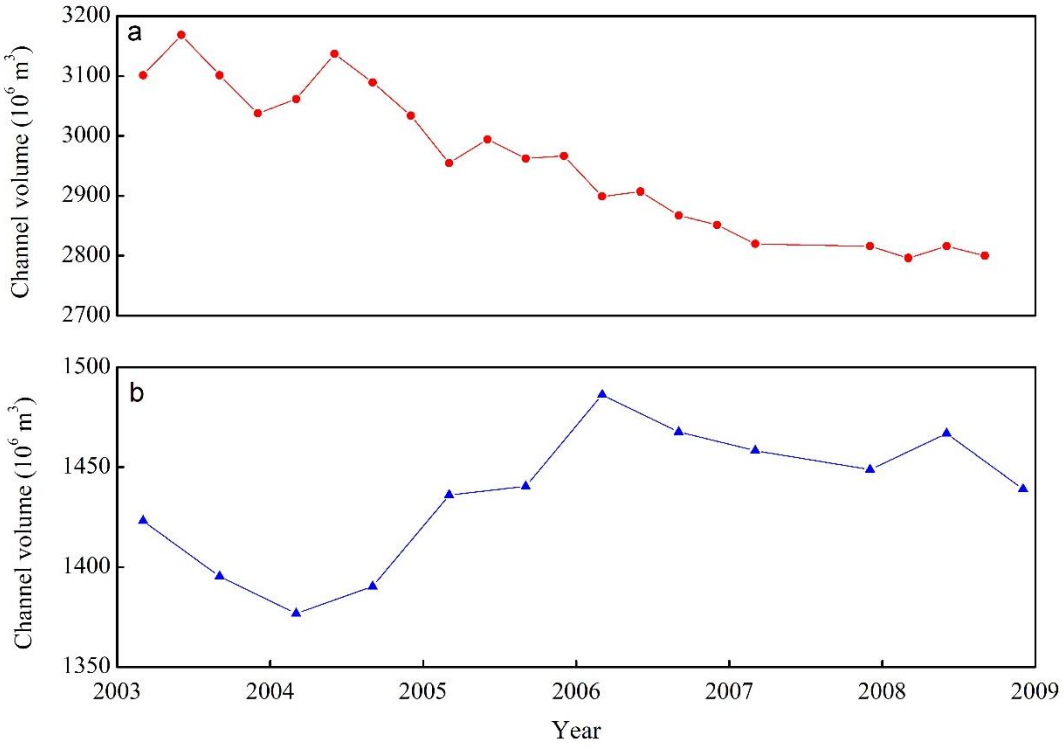

Fig.7. Variation of channel volume in two branching channels of the Yangtze Estuary after TGD impoundment in 2003. (a) Variation of channel volume below the water level of +2.00 m in the North Passage. (b) Variation of channel volume below the water level of 0.00 m in the South Passage. The water level is relative to the theoretical low-tide datum at Wusong (Fig.1b).

6. CONCLUSIONS

The present study reveals that the heavy deposition during 2002-2009 in the Yangtze Estuary was tightly related to the hydrologic shift from river flood events during 1997-2002 to low discharge events during 2002-2009 because the shift led to weaker ebb-tide force and relatively stronger flood-tide force in the

estuary. The sediment for the deposition mainly came from the offshore area, carried by the relatively strengthened flood-tide force.

The ebb partition ratios, namely, the seaward water excavating force in the north and south branching channels increase and decrease respectively as runoff discharge grows; this leads to more sediment deposition in the northern and southern subareas respectively with low and high $D_{60,000}$ values. Therefore, the heavy deposition mainly occurred in northern subareas due to the significant decreases and increases of ebb partition ratios in the north and south branching channels respectively when the runoff discharge diminished a lot during the hydrologic shift.

The ongoing construction of a cascade of large dams along the upper Yangtze will restrain natural hydrologic shifts between flood events and low discharge events in the watershed, and decrease the occurrence frequency of flood events; this subsequently promotes continuous deposition in the Yangtze Estuary. Meanwhile, the more deposition will continue to occur in the northern subareas.

The insights provided by this study should be useful for the design of future navigational projects and the planning of land resources in the Yangtze Estuary, and also might translate to other estuaries where fluvial water and sediment discharges are experiencing high degree of changes. A numerical model simulation will be carried out in the next step to quantify the impacts of fluvial discharges, tide, wave, storm surge and human interferences on the morphological evolution in the Yangtze Estuary.

ACKNOWLEDGEMENTS

This research is supported by the Scientific Research Project of Hunan Provincial Department of Education (No. 20B021), the Hunan Provincial Natural Science Foundation of China (No. 2021JJ40607 and No. 2020JJ5575), the National Key R&D Program of China (No. 2018YFC0407201) and the National Natural Science Foundation of China (No. 51779185). We highly appreciate the generosity of Changjiang Water Resources Commission for providing us the hydrologic data. The authors declare no competing financial or other conflicts of interest regarding the publication of this paper.

REFERENCES

Andrews, E. D., “Effective and bankfull discharges of streams in the Yampa River Basin, Colorado and Wyoming,” Journal of Hydrology, Vol.46(3-4), 311-330, 1980.

Crapoulet, A., Hequette, A., Marin, D., Levoy, F., and Bretel, P., “Variations in the response of the dune coast of northern France to major storms as a function of available beach sediment volume,” Earth Surface Processes and Landforms, Vol.42（11）, 1603-1622, 2017.

Dai, Z. J., Du, J. Z., Li, J. F., Li, W. H., and Chen, J. Y., “Runoff characteristics of the Changjiang River during 2006: Effect of extreme drought and the impounding of the Three Gorges Dam,” Geophysical Research Letters, Vol.35（7）, L07406, 2008.

Dai, Z. J., Fagherazzi, S., Mei, X. F., Chen, J. Y., and Meng, Y., “Linking the infilling of the North Branch in the Changjiang (Yangtze) estuary to anthropogenic activities from 1958 to 2013,” Marine Geology, Vol.379, 1-12, 2016.

Dai, Z. J., Liu, J. T., Wei, W., and Chen, J. Y., “Detection of the Three Gorges Dam influence on the Changjiang (Yangtze River) submerged delta,” Scientific Reports**,** Vol.4, 6600, 2014.

Dao, F. H., Luan, H. L., Yang, W. L., Ding, P. X., and Ge, J. Z., “Influence of the diversion project and bathymetric change of Ruifeng Shoal on the flow diversion ratios in the South and North Passage of Yangtze River Estuary,” Journal of East China Normal University (Natural Science), Vol.2018(3), 170-183, 2018. (in Chinese)

Day, J. W., Pont, D., Hensel, P. F., and Ibanez, C., “Impacts of sea-level rise on deltas in the Gulf of Mexico and the Mediterranean: The importance of pulsing events to sustainability,” Estuaries, Vol.18(4), 636-647, 1995.

Du, J. L., Yang, S. L., and Chen, G. P., “Influence of human activities on the evolution of the tidal flat of Yangtze River delta front during the last 30 years,” Marine Science Bulletin, Vol.32(3), 296-302, 2013. (in Chinese)

Duan, W. X., Guo, S. L., Wang, J., and Liu, D. D., “Impact of cascaded reservoirs group on flow regime in the middle and lower reaches of the Yangtze River,” Water, Vol.8(6), 1-21, 2016.

Emmett, W. W., and Wolman, M. G., “Effective discharge and gravel-bed rivers,” Earth Surface Processes Landforms, Vol.26(13), 1369-1380, 2001.

Fox, H. R., Wilby, R. L., and Moore, H. M., “The impact of river regulation and climate change on the barred estuary of the Oued Massa, southern Morocco,” Regulated Rivers-Research & Management, Vol.17(3), 235-250, 2001.

Gomez, B., Coleman, S. E., Sy, V. W. K., Peacock, D. H., and Kent, M., “Channel change, bankfull and effective discharges on a vertically accreting, meandering, gravel-bed river,” Earth Surface Processes and Landforms, Vol.32(5), 770-785, 2007.

Gao, M., Fan, Q. J., Tan, Z. W., and Zheng, W. Y., “Research on bifurcation ratio in the North Passage of Yangtze Estuary,” Port & Waterway Engineering, Vol.2009(5), 82-86, 2009. (in Chinese).

Grady, A. E., Moore, L. J., Storlazzi, C. D., Elias, E., and Reidenbach, M. A., “The influence of sea level rise and changes in fringing reef morphology on gradients in alongshore sediment transport,” Geophysical Research Letters, Vol.40(12), 3096-3101, 2013.

Guo, Z. G., Yang, Z. S., Fan, D. J., and Pan, Y. J., “Seasonal variation of sedimentation in the Changjiang Estuary mud area,” Journal of Geographical Sciences, Vol.13(3), 348-354, 2003.

He, Y. F., Chen, H. Q., and Chen, J. Y., “Morphological evolution of mouth bars on the Yangtze estuarine waterways in the last 100 years,” Journal of Geographical Sciences, Vol.23(2), 219-230, 2013.

Ji, Z. X., and Jiang, Z. X., “Impacts of sea level rise on coastal erosion in the Changjiang River delta and north Jiangsu coastal plain,” Chinese Geographical Science, Vol.4(4), 310-321, 1994.

Li, M. T., Chen, Z. Y., Yin, D. W., Chen, J., Wang, Z. H., and Sun, Q. L., “Morphodynamic characteristics of the dextral diversion of the Yangtze River mouth, China: tidal and the Coriolis Force controls,” Earth Surface Processes and Landforms, Vol.36(5), 641-650, 2011.

Li, S., Xiong, L. H., Dong, L. H., and Zhang, J., “Effects of the Three Gorges Reservoir on the hydrological droughts at the downstream Yichang station during 2003-2011,” Hydrological Processes, Vol.27(26), 3981-3993, 2013.

Liu, J., 2008, “Study on Morphological Evolution and Siltation in Deep Waterway due to Channel Re-construction in the North Passage, Yangtze Estuary,” PhD Thesis. State Key Laboratory of Estuarine and Coastal Research, East China Normal University, Shanghai, CA. (in Chinese)

Luan, H. L., Ding, P. X., Wang, Z. B., Ge, J. Z., and Yang, S. L., “Decadal morphological evolution of the Yangtze Estuary in response to river input changes and estuarine engineering projects,” Geomorphology, Vol.265, 12-23, 2016.

Milliman, J. D., “Blessed dams or damned dams,” Nature**,** Vol.388, 325-326, 1997.

Rangel-Buitrago, N., and Anfuso, G. (2011). “Coastal storm characterization and morphological impacts on sandy coasts,” Earth Surface Processes and Landforms, Vol.36(15), 1997-2010, 2011.

Rao, K. N., Subraelu, P., Kumar, K. C. V. N., Demudu, G., Malini, B. H., Rajawat, A. S., and Ajai. (2010). “Impacts of sediment retention by dams on delta shoreline recession: evidences from the Krishna and Godavari deltas, India,” Earth Surface Processes and Landforms, Vol.35(7), 817-827, 2010.

Ren, M. E., Zhang, R. S., and Yang, J. H. (1985). “Effect of Typhoon No-8114 on coastal morphology and sedimentation of Jiangsu Province, Peoples-Republic-of-China,” Journal of Coastal Research, Vol.1(1), 21-28, 1985.

Shepard, F. P., 1963, “Submarine Geology,” Harper & Row: New York.

Sherwood, C. R., Jay, D. A., Harvey, R. B., Hamilton, P., and Simenstad, C. A., “Historical changes in the Columbia River Estuary,” Progress in Oceanography, Vol.25(1), 299-352, 1990.

Song, D. H., and Wang, X. H., “Suspended sediment transport in the Deepwater Navigation Channel, Yangtze River

Estuary, China, in the dry season 2009: 2. Numerical simulations," Journal of Geophysical Research-Oceans, Vol.118(10), 5568–5590, 2013.

Song, D. H., Wang, X. H., Cao, Z. Y., and Guan, W. B., "Suspended sediment transport in the Deepwater Navigation Channel, Yangtze River Estuary, China, in the dry season 2009: 1. Observations over spring and neap tidal cycles," Journal of Geophysical Research-Oceans, Vol.118(10), 5555–5567, 2013.

Stanley, D. J., and Warne, A. G., "Nile delta – recent geological evolution and human impact," Science, Vol.260(5108), 628-634, 1993.

van Puijenbroek, M. E. B., Limpens, J., de Groot, A. V., Riksen, M. J. P. M., Gleichman, M., Slim, P. A., van Dobben, H. F., and Berendse, F., "Embryo dune development drivers: beach morphology, growing season precipitation, and storms," Earth Surface Processes and Landforms, Vol.42(11), 1733-1744, 2017.

Wei, W., Tang, Z. H., Dai, Z. J., Lin, Y. F., Ge, Z. P., and Gao, J. J., "Variations in tidal flats of the Changjiang (Yangtze) estuary during 1950s-2010s: Future crisis and policy implication," Ocean & Coastal Management, Vol.108(SI), 89-96, 2015.

Wu, H. L., Shen, H. T., and Wang, Y. H., "Evolution of mouth bars in the Changjiang Estuary, China: A GIS supporting study," In International Conference on Estuaries and Coasts, Hangzhou, CA.

Wu, Y., "Evolution of distributary reach of south and north channels in the Yangtze Estuary and influence on surrounding regulation projects," Port & Waterway Engineering, Vol.2017(7), 136-140, 2017. (in Chinese)

Xia, J. Q., Li, X. J., Zhang, X. L., and Li, T. , "Recent variation in reach-scale bankfull discharge in the Lower Yellow River," Earth Surface Processes and Landforms, Vol.39(6), 723-734, 2014.

Xu, Y., and Zhu, Z., "Study and practice of comprehensive utilization of dredging soil of the Yangtze Estuary Deepwater Channel Engineering," Port & Waterway Engineering, Vol.2009(4), 127–133, 2009. (in Chinese)

Yang, S. L., Friedrichs, C. T., Shi, Z., Ding, P. X., Zhu, J., and Zhao, Q. Y., "Morphological response of tidal marshes, flats and channels of the outer Yangtze River mouth to a major storm," Estuaries**,** Vol.26(6), 1416-1425, 2003.

Yang, S. L., Zhao, Q. Y., Xie, W. H., and Wang, X. F., "Forecast of impacts of sea-level rise on the low colonized islands and their surrounding waters in the Changjiang River mouth," Chinese Geographical Science, Vol.10(2), 113-118, 2000.

Yang, Y. P., 2014, "Impact of water-sediment condition variation on geomorphic system in Yangtze Estuary," PhD Thesis. State Key Laboratory of Water Resources and Hydropower Engineering Science, Wuhan University, Wuhan, CA. (in Chinese)

Yang, Y. P., Li, Y. T., Sun, Z. H., and Fan, Y. Y.,

"Suspended sediment load in the turbidity maximum zone at the Yangtze River Estuary: The trends and causes," Journal of Geographical Sciences, Vol.24(1), 129-142, 2014.

Yun, C. X., 2004, "Recent Developments of the Changjiang Estuary," China Ocean Press, Beijing. (in Chinese)

Zhang, M., Townend, I., Zhou, Y. X., and Cai, H. Y., "Seasonal variation of river and tide energy in the Yangtze estuary, China," Earth Surface Processes and Landforms, Vol.41(1), 98-116, 2016.

Zhang, X. D., Yang, Z. S., Zhang, Y. X., Ji, Y., Wang, H. M., Lv, K., and Lu, Z. Y., "Spatial and temporal shoreline changes of the southern Yellow River (Huanghe) Delta in 1976-2016," Marine Geology, Vol.395, 188-197, 2018.

Zhao, J., Guo, L. C., He, Q., Wang, Z. B., van Maren, D. S., and Wang, X. Y., "An analysis on half century morphological changes in the Changjiang Estuary: Spatial variability under natural processes and human intervention," Journal of Marine Systems, Vol.181, 25-36, 2018.

Zhou, X. Y., Zheng, J. H., Doong, D. J., and Demirbilek, Z., "Sea level rise along the East Asia and Chinese coasts and its role on the morphodynamic response of the Yangtze River Estuary," Ocean Engineering, Vol.71, 40-50, 2013.

Zhu, B. Y., Li, Y. T., Yue, Y., and Yang, Y. P., "Aggravation of north channels' shrinkage and south channels' development in the Yangtze Estuary under dam-induced runoff discharge flattening," Estuarine Coastal and Shelf Science, Vol.187, 178-192, 2017.